Molecular weight of polyethylenimine-dependent transfusion and selective antimicrobial activity of functional silver nanoparticles

Atul Kumar Tiwari[1], Munesh Kumar Gupta[2], Govind Pandey[3], Roger J. Narayan[4,a)], Prem C. Pandey[1,a)] (iD)

[1]Department of Chemistry, Indian Institute of Technology, Varanasi, Uttar Pradesh 221005, India
[2]Department of Microbiology, Institute of Medical Sciences, Banaras Hindu University, Varanasi, Uttar Pradesh 221005, India
[3]Department of Pediatrics, King George Medical University, Lucknow, Uttar Pradesh 226003, India
[4]Department of Biomedical Engineering, North Carolina State University, North Carolina 27695, USA
[a)]Address all correspondence to this authors. e-mail: rjnaraya@ncsu.edu and pcpandey.apc@iitbhu.ac.in

Synthetic cationic polymer-mediated synthesis of silver nanoparticles and selective antimicrobial activity of the same were demonstrated. Polyethyleneimine (PEI)-coated silver nanoparticles showed antimicrobial activity against *Acinetobacter baumannii* as a function of the polymeric molecular weight (MW) of PEI. Silver nanoparticles were coated with PEI of three different MWs: Ag-NP-1 with PEI exhibiting a MW of 750,000, Ag-NP-2 with PEI exhibiting a MW of 1300, and Ag-NP-3 with PEI exhibiting a MW of 60,000. These nanoparticles showed a particle size distribution of 4–20 nm. The nanoparticles exhibited potent antimicrobial activity against *A. baumannii*, with the minimum inhibitory concentration of Ag-NP-1, Ag-NP-2, and Ag-NP-3 on the order of 5, 10, and 5 µg/mL, respectively, and minimum bactericidal concentration of Ag-NP-1, Ag-NP-2, and Ag-NP-3 on the order of 10, 20, and 10 µg/mL, respectively. Fluorescence imaging of Ag-NPs revealed selective transfusion of Ag-NPs across the cell membrane as a function of the polymeric MW; differential interaction of the cytoplasmic proteins during antimicrobial activity was observed.

INTRODUCTION

The technologies for introducing a cationic charge on inorganic materials (including nanoparticles) typically involve surface grafting with amine groups and coating with cationic polymers (e.g., polyethyleneimine (PEI), poly-amidoamine, and poly-lysine) through either covalent or electrostatic association [1,2,3]. PEIs are synthetic cationic polymers that compact DNA and siRNA into complexes, which are taken up in cells [3]. Since the cytotoxicity of PEI coating can interfere with the efficacy of the delivery system, it is possible that by selecting optimal polymeric lengths to control transfusion efficiency, one may simultaneously reduce or eliminate toxic effects of cationic polymer-coated nanoparticles. In turn, this directed us to investigate the synthesis and coating of silver nanoparticles (Ag-NPs) by PEI as a function of polymeric molecular weight (MW) [4,5].

We are interested in the interaction of PEI-coated Ag-NPs with multidrug-resistant (MDR) microbes [5,6,7,8]. Silver is

considered to be a Lewis acid [9], which has the tendency to react with a Lewis base; Lewis bases include phosphorous- and sulfur-containing biomolecules, the major components of the cell membrane, proteins, and DNA bases. Hence, Ag-NPs can accumulate on the cell membrane and cause morphological changes such as shrinkage of the cytoplasm, membrane detachment, and the formation of numerous electron-dense pits, resulting in the disruption of the cell membrane [7,10,11]. A cationic polymer coating may allow for the selective transfusion of silver nanoparticles.

We have already demonstrated that PEI along with an organic reducing agent allows for controlled synthesis of gold nanoparticles [12]. Since the amine functionality of cationic polymer enables microwave activity, it is desirable to control the reduction of the noble metal cation under microwave incubation. Interestingly, we have observed rapid synthesis of PEI-coated silver nanoparticles within less than 1 min under

microwave incubation. In addition, the process of nanoparticle formation may further be controlled as a function of MW of the synthetic polymer. The antimicrobial activity of the nanoparticles was examined using *Acinetobacter baumannii,* which is the predominant cause of hospital-acquired infections in intensive care unit-admitted patients; clinical manifestations of infection include pneumonia, bacteremia, wound infections, and urinary tract infection. The antimicrobial activity of several new types of nanomaterials has recently been demonstrated. For example, Matharu et al. demonstrated the antimicrobial activity of tungsten nanoparticles and tungsten nanocomposite fibers against bacteriophage T4, Escherichia coli, and Staphylococcus aureus [13]; the antimicrobial activity of graphene nanoparticles was also recently demonstrated [14].

One recent study demonstrated that fluorescence imaging can be used to understand protein–nanoparticle interactions [15]. Silver nanoparticles with cationic polymers may alter either intrinsic fluorescence of surface-active proteins or maintain high transfusion efficiency across the bacterial cell membrane; the fluorescence behavior of cytoplasmic fluorescent biomolecules may provide insight in this process. The wide variation in PEI MW between 1300 and 75,000 may allow for the selective transfusion of PEI-coated Ag-NPs across the bacterial cell membrane. Indeed, valuable information on the impact of cationic polymeric MW on antimicrobial activity may be obtained. The antibacterial activity of the Ag-NPs [7,16] as detected by fluorescence imaging may be attributed to surface-binding properties, active biomolecule/ion release, and/or generation of high oxidative stress [7,17,18] as a function of the polymeric coating on the silver nanoparticles. In this study, fluorescence imaging of PEI-coated Ag-NPs with three different MWs was used to understand nanoparticle–*Acinetobacter baumannii* cell membrane interactions, specifically antimicrobial activity, as a function of PEI MW.

RESULTS AND DISCUSSION

Polyethylenimine-mediated synthesis of silver nanoparticles

PEI-mediated synthesis of gold nanoparticles under ambient conditions has been studied in detail [12]. The PEI-capped silver cation allowed microwave-assisted reduction of silver cations in the presence of an organic reducing agent, namely cyclohexanone or formaldehyde, leading to the formation of three different silver nanoparticles. Figure 1(A) shows the formation of silver nanoparticles coated with PEI of three different MWs, such as Ag-NP-1, Ag-NP-2, and Ag-NP-3. Figure 1(Aa) shows the results recorded from Ag-NP-1, Fig. 1(Ab) shows the results recorded from Ag-NP-2, and Fig. 1(Ac) shows the results recorded from Ag-NP-3. The process allowed for rapid formation of Ag-NPs regardless of MW. The properties

of Ag-NP-1, Ag-NP-2, and Ag-NP-3 differed as a function of MW. The concentration of PEI also affected the synthesis of Ag-NPs. The Ag-NPs were characterized by transmission electron microscopy (TEM) [Fig. 1(B)] and by zeta potential measurements [Fig. 1(C)].

Bactericidal activity, minimum inhibitory concentration, and minimum bactericidal concentration of Ag-NPs

The three Ag-NPs showed bactericidal activity against *A. baumannii*; a variation in bactericidal activity was noted on the basis of MW [Fig. 2(a)]. The minimum inhibitory concentration (MIC) and minimum bactericidal concentration (MBC) values of each silver nanoparticle (Ag-NP) were determined by the broth microdilution method in flat bottom sterile microtiter plates. The MBC values for Ag-NP-1, Ag-NP2, and Ag-NP3 against the strain of *A. baumannii* were 5, 10, and 5 µg/mL, respectively. The MBC values for Ag-NP-1, Ag-NP2, and Ag-NP3 were 10, 20, and 10 µg/mL, respectively [Fig. 2(b)]. It was observed that the antibacterial activity of Ag-NPs depends on the MW of PEI (Fig. 2). Furthermore, it was observed that Ag-NPs capped with high-molecular-weight PEI had more potent bactericidal activity than Ag-NPs capped with low-molecular-weight PEI. The differential bactericidal activity may be attributed to the differences in branching of PEI among the samples; the highly branched PEI (MW 750,000)-capped Ag-NPs (Ag-NP-1) and moderate branched PEI (MW 60,000)-capped Ag-NPs (Ag-NP-4) showed lower MIC values than unbranched PEI (MW 1300)-capped Ag-NPs (Ag-NP-2). As such, it appears that branched PEI interacts more stably with the outer membrane of *A. baumannii*, which in turn destabilizes the bacterial cell membrane.

Dynamic fluorescence quenching of fluorescein by PEI-capped Ag-NPs

It has previously been demonstrated that the bactericidal ability of Ag-NPs is potentiated by light [13]. The photosensitization phenomenon was explored to understand the dynamic interaction between silver nanoparticles and proteins. To trigger light emission, we chose to utilize fluorescein, which shows emission in the visible range. Silver nanoparticles showed good quenching of fluorescence; as such, fluorescence imaging was used to understand protein–nanoparticle interactions. In the present work, we have analyzed the quenching behavior of PEI-capped Ag-NPs in the presence and absence of *A. baumannii*; fluorescein was used as a fluorophore in these studies. It was observed that as-synthesized Ag-NPs quenched the intrinsic fluorescence of fluorescein molecules by nearly 60% [Figs. 3(A) and 3(B)]. However, when cells (10^4 cells) were
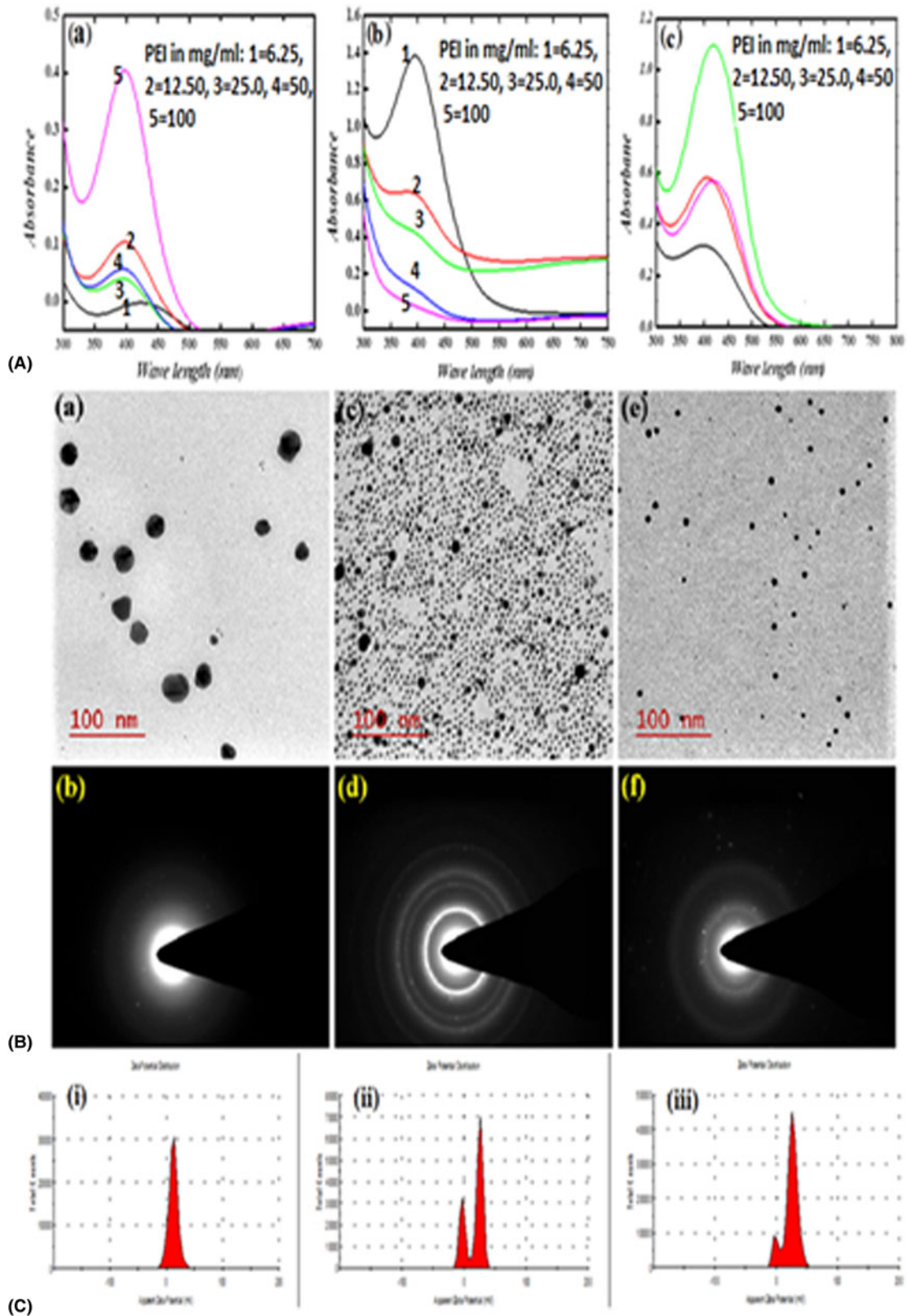
Figure 1: (A) UV–Vis spectra of (a) Ag-NP-1, (b) Ag-NP-2, and (c) Ag-NP-3. (B) TEM images along with the respective SAED pattern of (a, b) Ag-NP-1, (c, d) Ag-NP-2 and (e, f) Ag-NP-3. (C) Zeta potential of (i) Ag-NP-1, (ii) Ag-NP-2, and (iii) Ag-NP-3.
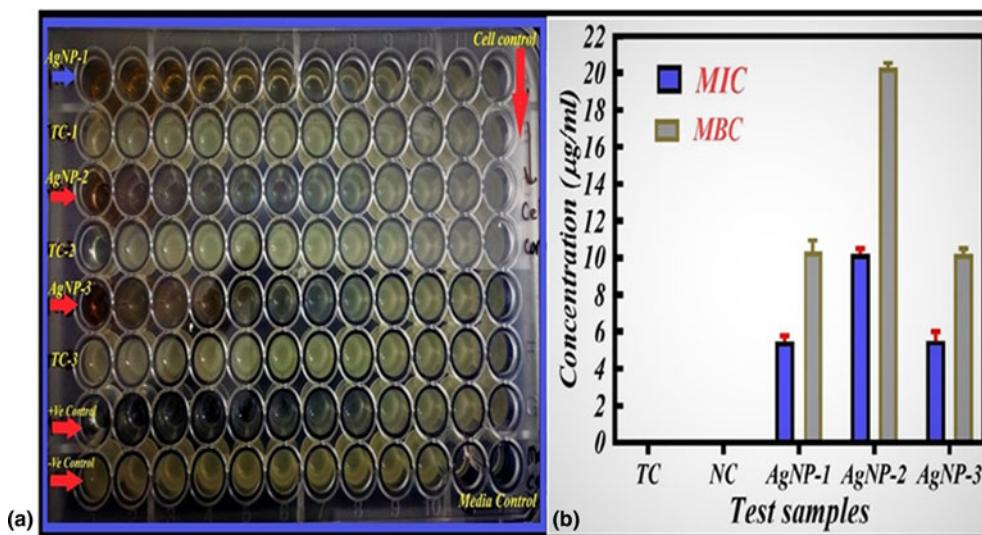
Figure 2: (a) The antibacterial property assessment plate. (b) MIC and MBC (μg/mL) values of each Ag-NPs against *A. baumannii* planktonic cells. TC represents test control and NC represents negative control.

added in the media, the quenching percentage decreased significantly to 40% (with an associated increase in cell number). The quenching subsequently decreased to 10%. In order to understand the quenching dynamics of the Ag-NPs, 3D fluorescence spectra [Fig. 3(C)] were recorded; the results of these studies indicate that Ag-NPs show more affinity toward cell surface-expressed proteins than fluorescein molecules in a cell number-dependent manner. The mechanism of this dynamic quenching behavior of Ag-NPs is shown in Scheme 1.

Cell surface interaction and membrane breakage of *A. baumannii* cells by Ag-NPs

The 2D (Fig. 4) and 3D (Fig. 5) intrinsic fluorescence spectra of standard protein bovine serum albumin (BSA) and *A. baumannii* cells were recorded using EEM at 280/300 nm with control and after treatment with Ag-NPs with several MWs for 1 or 3 h. It was observed that in the control system, standard protein BSA and *A. baumannii* cells showed an intrinsic fluorescence emission on 330 nm (the peak associated with tryptophan); no other emission peak was observed. After treatment with PEI-capped Ag-NPs for 1 h, it was observed that Ag-NP-2 interacted very quickly with tryptophan residues of BSA and cell surface-expressed proteins; as a result, tyrosine residues (with a peak at 310 nm) were exposed, followed by denaturation of the quaternary structure of the protein. Ag-NP-1 and Ag-NP-3 showed similar interactions with BSA and cells; quenching in the intrinsic fluorescence of proteins up to 60% and partial denaturation were observed [Figs. 4(ai,ii) and 5 (a)]. Furthermore, when the incubation time was increased to 3 h [Fig. 4(bi,ii)], the dynamics of interaction with BSA

was changed; Ag-NP-1, Ag-NP-2, and Ag-NP-3 showed denaturation of the quaternary structure of the protein, exposing tyrosine residues. Moreover, in the presence of *A. baumannii*, Ag-NP-1 and Ag-NP-3 showed greater quenching in fluorescence; Ag-NP-2 completely denatured the surface proteins. In order to understand cell membrane damage, cells were incubated for 6 h with different Ag-NPs; centrifugation of the cell-containing solution was performed; fluorescence spectroscopy (EX/EM at 280/300 nm) of the supernatant was recorded as shown in Fig. 6. It was found that all three Ag-NPs caused partial and complete denaturation of proteins, indicating cell membrane breakage.

The possible mechanism of membrane breakage is that Ag-NP-1s exhibit a larger size and a higher cationic activity in comparison to Ag-NP-2s and Ag-NP-3s. In turn, Ag-NP-1s are unable to pass the outer membrane and interfere with membrane potential, denaturing the surface-expressed proteins; this process results in the generation of reactive oxygen species, followed by an oxidative burst by the cell. Ag-NP-2s and Ag-NP-3s are smaller in size and have lower MWs; these particles can pass easily through the outer membrane via porins. They can enter the cell via channels and interact with both cytoplasmic proteins and transmembrane proteins, resulting in the collapse of cellular physiology (Scheme 2).

Accordingly, polymeric MW plays a central role not only in the synthesis of silver nanoparticles, but also in the selective transfusion ability of Ag-NPs across the cytoplasmic wall. The Ag-NP-2s made with PEI exhibiting a MW of ~1300 allow high efficiency of Ag-NP-2 transfusion and selective interaction with cytoplasmic biomolecules (as evidenced from the fluorescence imaging, which revealed an additional
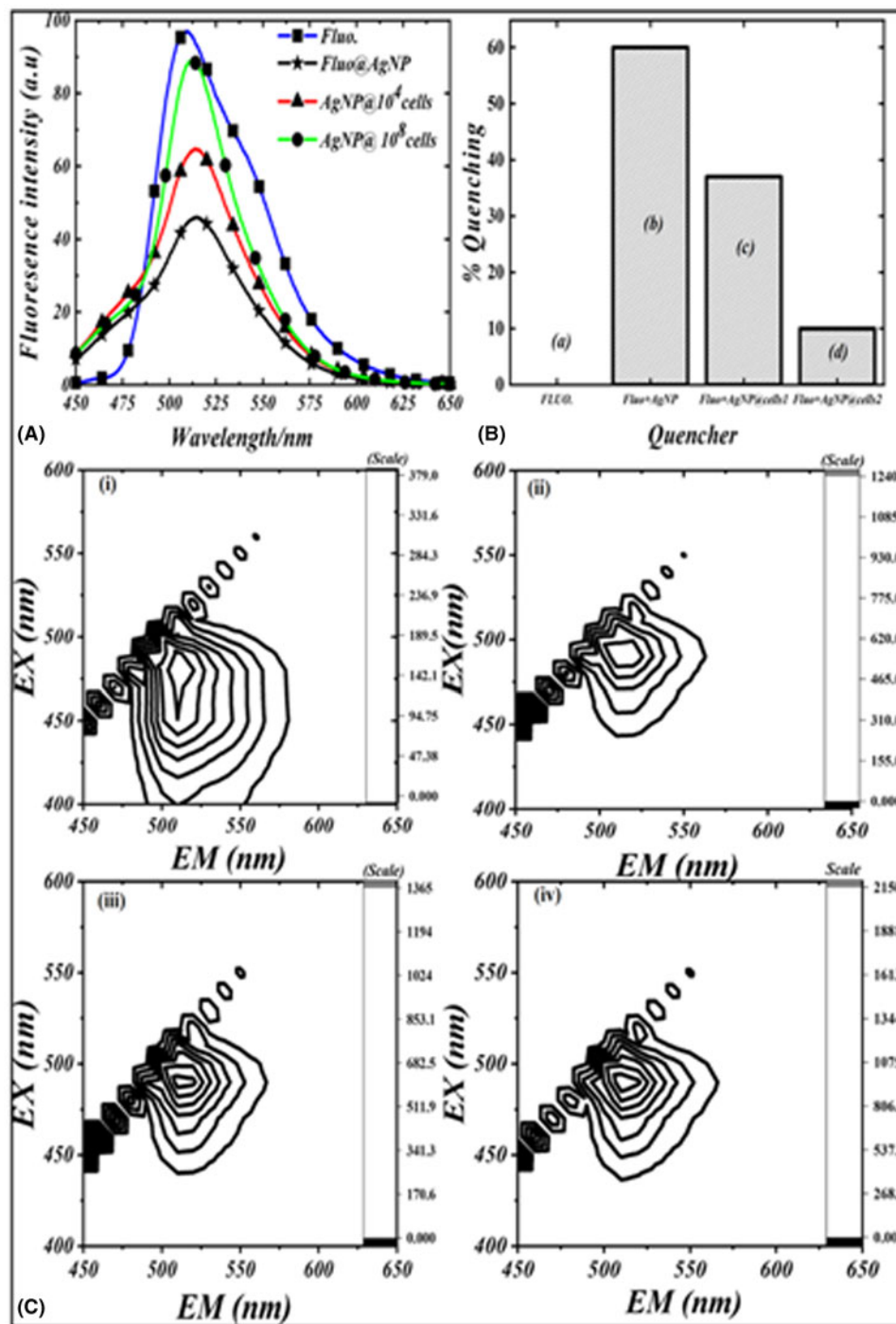
Figure 3: (A) 2D fluorescence dynamic quenching of fluorescein by PEI-capped Ag-NP in the absence and presence of *A. baumannii* cells. (B) Bar diagram showing % quenching and dequenching of fluorescein by Ag-NP: (a) control, (b) in the presence of Ag-NP, (c) on the addition of 10^4 cells, and (d) on the addition of 10^8 cells. (C) 3D fluorescence imaging on dynamic quenching of fluorescein by Ag-NP: (i) control, (ii) in the presence of Ag-NP and the absence of cell, and (iii) in the presence of 10^4 cells and in the presence of 10^8 cells.

fluorescence peak between 420 and 440 nm). The impact of the cationic polymeric weight on selective movement of Ag-NP-2 and Ag-NP-3 across the cytoplasmic membrane as described in this manuscript has not previously been described.

The toxicity of silver nanoparticles is an important parameter that affects the clinical use of these materials; the findings on the stability of silver nanoparticles during antimicrobial action seem to be quite reasonable. The earlier finding
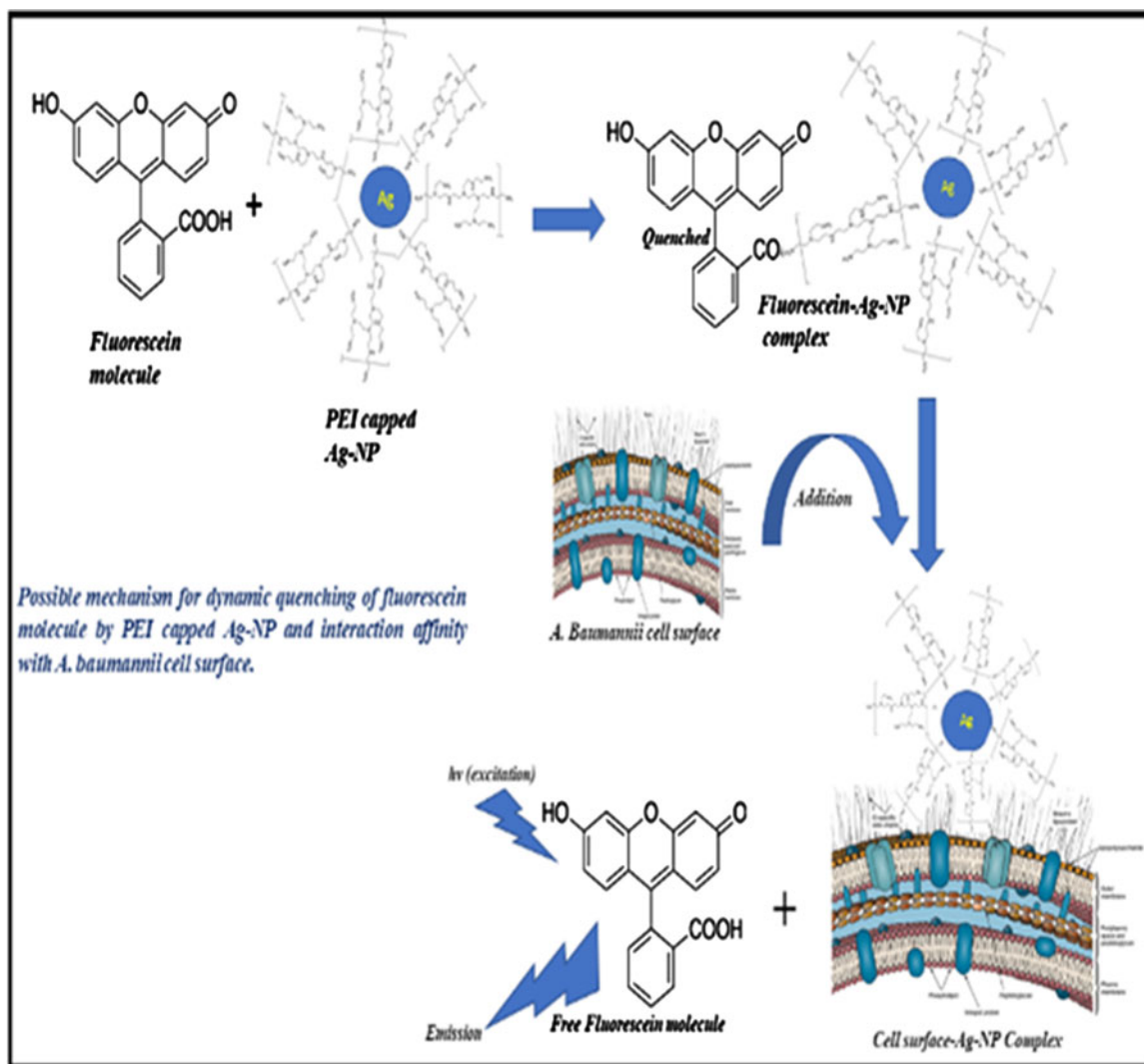
Scheme 1: Mechanism showing the possible dynamic quenching behavior of PEI-capped Ag-NPs to fluorescein and interaction with *A. baumannii*.

demonstrated that AgNP affects the cell wall; it does not kill the cell [19]. In addition, the study indicated that AgNP is not toxic to the E. coli K-12 strain, whereas silver ions showed potent toxicity under similar conditions [20]. These previous studies directed the current evaluation of AgNP function. Overall, in environmental assessments, considerations of the combined toxicity of dissimilar NPs will allow more accurate assessments of their environmental risks.

CONCLUSIONS

The synthesis and antimicrobial activity of cationic polymer-coated Ag-NPs as a function of polymeric MW was reported in the present study. Selective transfusion of Ag-NPs across the cell membrane was observed; the Ag-NPs interfered with the membrane integrity by interacting with surface-expressed proteins and showed antimicrobial efficiency based on MW.

A new fluorescence peak was noted for PEI with a MW of 1300; this feature was absent when similar observations were recorded using Ag-NPs made using PEI with MWs of 750,000 and 60,000; this work indicates that the hydrodynamic radius of the AgNPs affects the transfusion of the AgNPs in *A. baumannii*.

MATERIALS AND METHODS

Materials

All MW PEI, silver nitrate (AgNO₃), fluorescein, and bovine serum albumin were obtained from Sigma Aldrich (Bangalore, Karnataka, India). Bacterial culture media such as Muller Hinton Broth (MHB), Muller Hinton Agar (MHA), and Nutrient Broth (NB) were purchased from Hi-Media Laboratories Ltd. (Mumbai, Maharashtra, India). Plasticware was purchased from Tarsons Product Pvt. Ltd. (Kolkata, West Bengal, India). The antibiotics
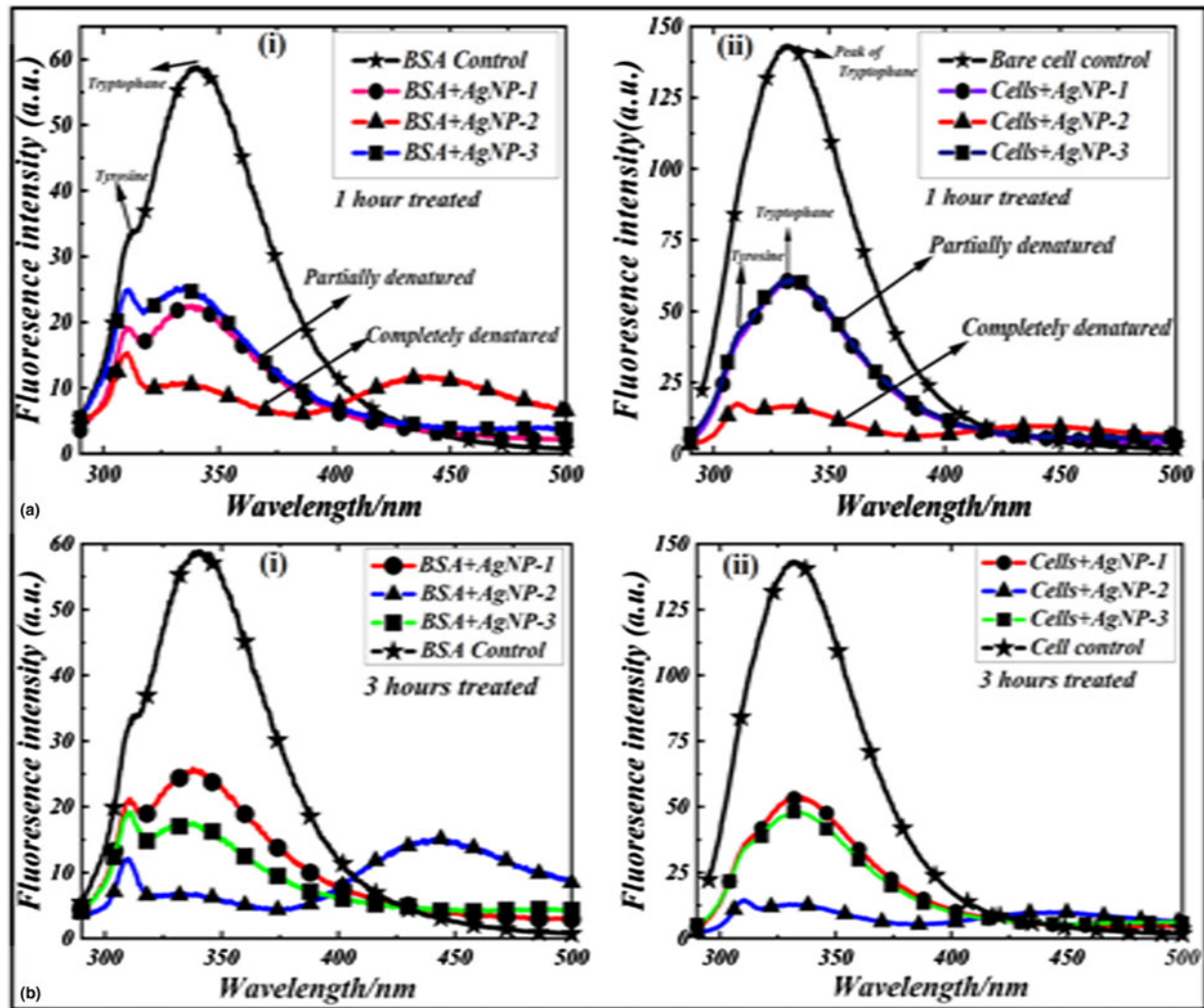
Figure 4: (a) (i) 2D fluorescence spectra of BSA and Ag-NP-1, Ag-NP-2, and Ag-NP-3 incubated for 1 h. (ii) 2D fluorescence spectra of *A. baumannii* and Ag-NP-1, Ag-NP-2, and Ag-NP-3 incubated for 1 h along with control. (b) (i) 2D fluorescence spectra of BSA and Ag-NP-1, Ag-NP-2, and Ag-NP-3 incubated for 3 h. (ii) 2D fluorescence spectra of *A. baumannii* and Ag-NP-1, Ag-NP-2, and Ag-NP-3 incubated for 3 h along with control.

and other routine chemicals were purchased from Sigma Aldrich (St. Louis, MO, USA). The organic solvents were purchased from Merck Life Science Private Limited (Bangalore, Karnataka, India). All of the reagents were analytical grade.

Bacterial strain

We have isolated one strain of *A. baumannii* from the endotracheal tube secretions of one ICU-admitted male patient who developed ventilator-associated pneumonia. This strain was identified based on the culture characteristics on MacConkey agar, blood agar, and Gram stain. Biochemical tests included catalase, oxidase, sugar fermentation test, and citrate utilization test. On antibiotic susceptibility testing, this strain was only sensitive to polymyxin B; it showed resistance to the other tested antibiotics, which include amoxicillin-clavulanic acid, ceftazidime, gentamycin, amikacin, ciprofloxacin, levofloxacin,

ampicillin-sulbactam, piperacillin-tazobactam, and the carbapenem group of antibiotics.

Synthesis of PEI-functionalized silver nanoparticles

PEI-1 (MW 750,000) and cyclohexanone-mediated synthesis of Ag-NP-1

Ethylene glycol (120 μL) and a methanolic solution of 1-vinyl 2-pyrrolidone (50 μL of a 250 mM solution) were placed in 2 mL glass vial, followed by the addition of a methanolic solution of $AgNO_3$ (10 μL of a 10 mM solution), PEI (150 μL of a 100 mg/mL solution), and cyclohexanone (20 μL). The reaction mixture was thoroughly mixed on a vortex mixer for 30 s and placed in a microwave oven for 15 s. The cycle was repeated four to six times in the microwave oven, resulting in the appearance of a deep yellow color that indicated the formation of Ag-NP-1.
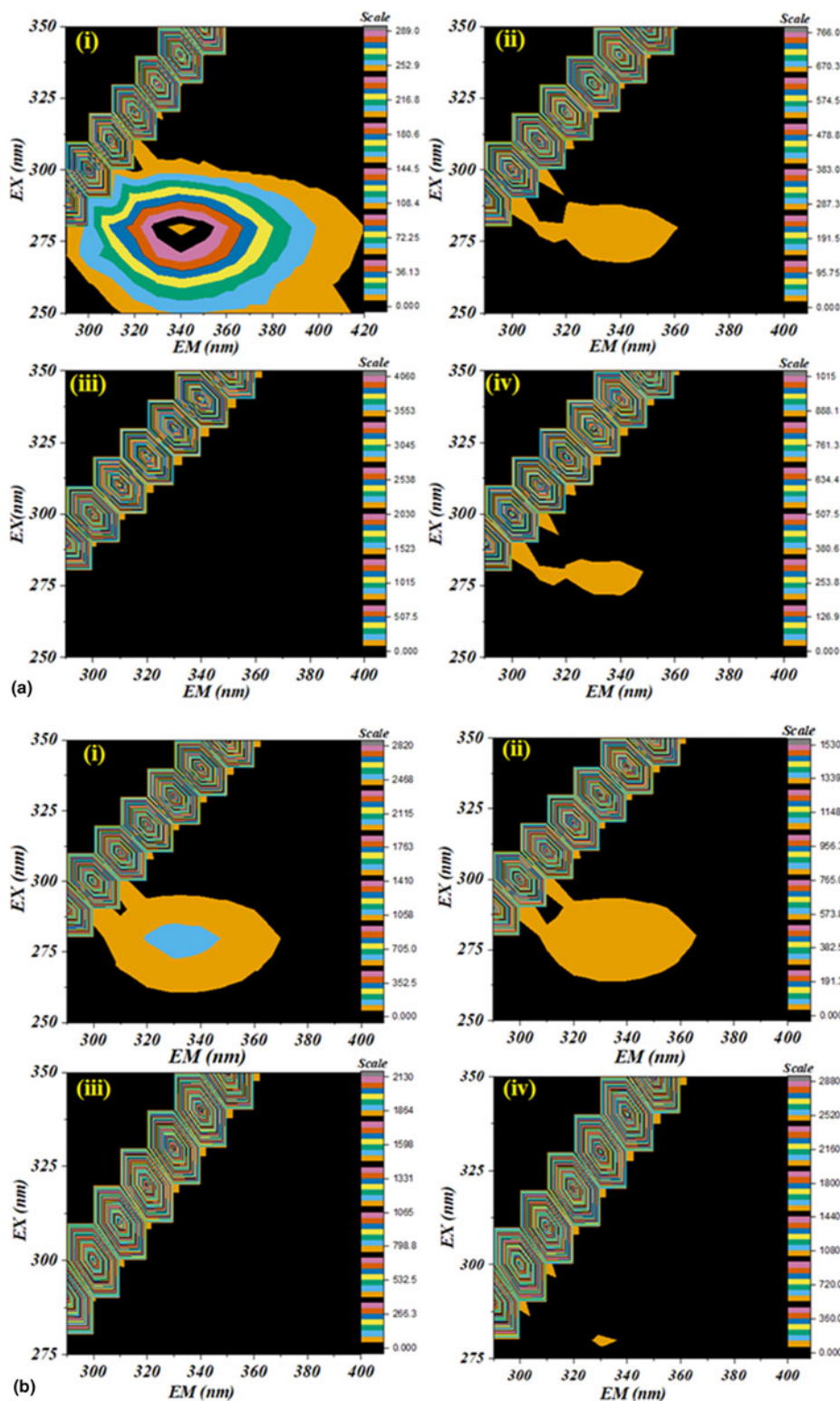
Figure 5: (a) 3D fluorescence contour plot of BSA (5 µg/mL) in the absence of Ag-NP and after incubation for 1 h at room temperature with (i) Ag-NP-1, (ii) Ag-NP-2, and (iii) Ag-NP-3. (b) 3D fluorescence contour plot of *A. baumannii* cells (10⁶ cells/mL): (i) in the absence of Ag-NPs and after incubation for 1 h at room temperature with (ii) Ag-NP-1, (iii) Ag-NP-2, and (iv) Ag-NP-3.

PEI-2 (MW 1300) and formaldehyde-mediated synthesis of Ag-NP-2

Ethylene glycol (120 µL) and a methanolic solution of 1-vinyl 2-pyrrolidone (50 µL of a 25 mM solution) were placed in a

2 mL glass vial, followed by the addition of a methanolic solution of AgNO₃ (10 µL of a 10 mM solution), PEI (20 µL of a 6.25 mg/mL solution), and formaldehyde (10 µL). The reaction mixture was thoroughly mixed on a vortex mixer for 30 s and
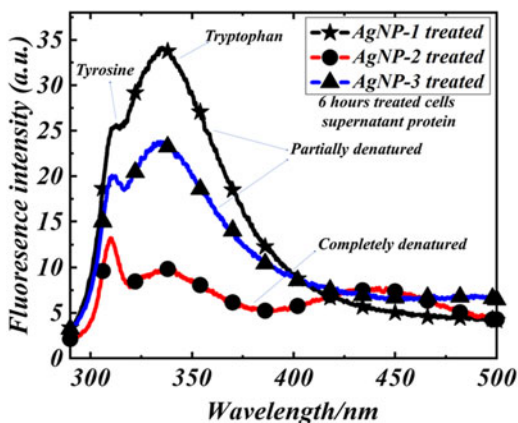
Figure 6: 2D fluorescence spectra of the supernatant obtained after centrifugation of the reaction mixture of *A. baumannii* cells (10^6 cells/mL) after incubation with Ag-NP-1, Ag-NP-2, and Ag-NP-3.

placed in a microwave oven for 15 s. The cycle was repeated two to five times in a microwave oven, resulting in the appearance of a deep yellow color that indicated the formation of Ag-NP-2.

PEI-3 (MW 60,000) and cyclohexanone-mediated synthesis of Ag-NP-3

Ethylene glycol (120 µL) and a methanolic solution of 1-vinyl 2-pyrrolidone (50 µL of a 50 mM solution) were placed in 2 mL glass vial, followed by the addition of a methanolic solution of AgNO₃ (10 µL of a 10 mM solution), PEI-3 (16.4 mg/mL; 100 µL), and cyclohexanone (20 µL). The reaction mixture was thoroughly mixed on a vortex mixer for 30 s and placed in a microwave oven for 15 s. The cycle was repeated two to three times in a microwave oven, resulting in the appearance of a deep brown color that indicated the formation of Ag-NP-3.

Characterization of functionalized Ag-NPs

All of the Ag-NPs were characterized using a U-2900 UV-Vis spectrometer (Hitachi, Tokyo, Japan) over the scan range of 250–800 nm. Transmission electron microscopy and electron diffraction (SAED) analysis of Ag-NPs was carried out using a Tecnai G2 20 Twin instrument (FEI, Hillsboro, OR, USA) at the IIT(BHU) Central Instrumentation Facility. Samples
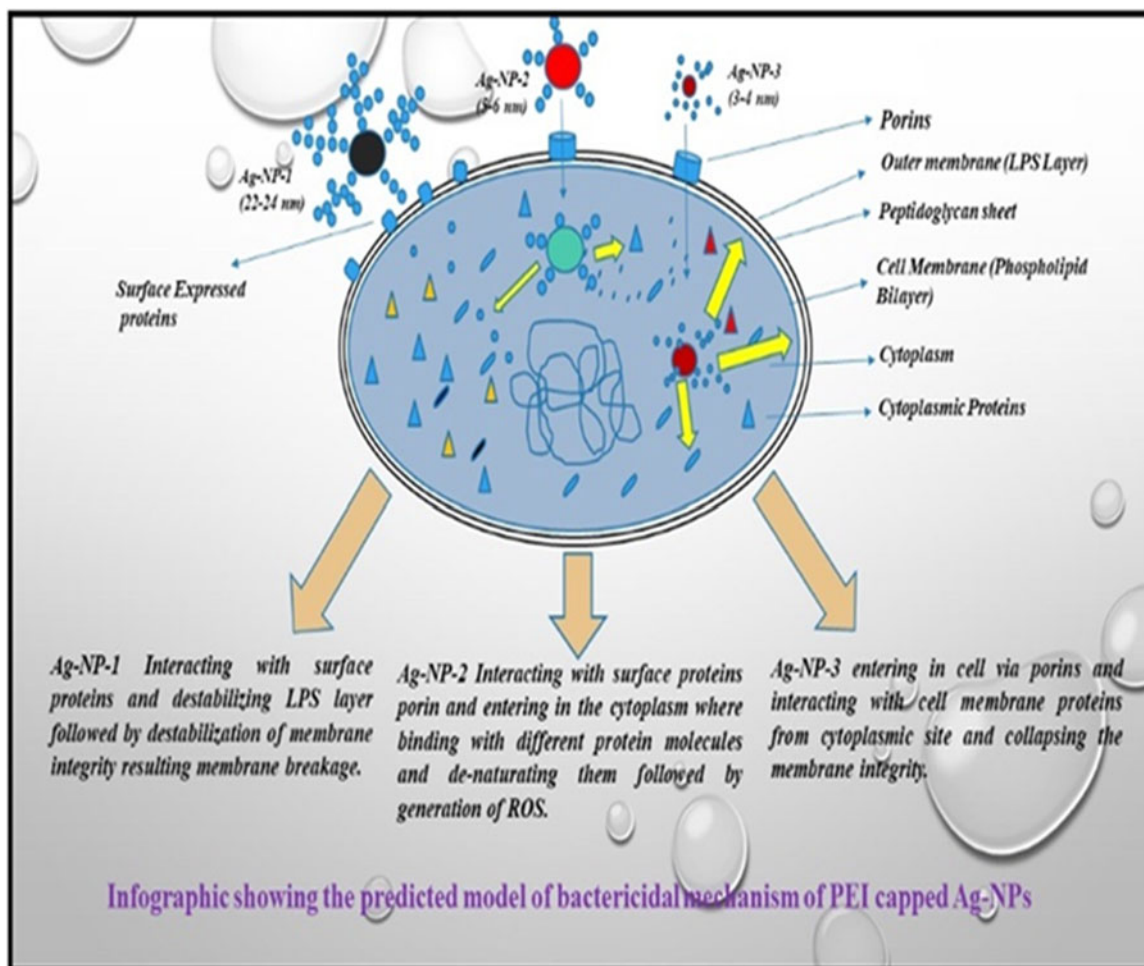
Scheme 2: Model of the possible bactericidal mechanism of Ag-NP-1, Ag-NP-2, and Ag-NP-3 against *A. baumannii*.

were prepared by diluting the Ag-NPs in methanol and drop-casting the solution on carbon-coated copper grids of 300 mesh. Zeta potential analysis was performed using a Zetasizer instrument (Malvern Panalytical, Malvern, UK).

Assessment of antibacterial activity and MIC and MBC determinations of Ag-NPs

The silver nanoparticles were evaluated for their activity against *A. baumannii* using the 2-fold serial dilution method [21]. The MIC and MBC values of synthesized Ag-NPs against *A. baumannii* were determined using the broth microdilution method in a flat bottom sterile 96-well microtiter plate as described previously [22,23,24]. In short, an overnight grown culture of *A. baumannii* in MHB medium was centrifuged; the obtained pellet was resuspended in fresh MHB medium for 4 h to achieve log phase at 37 °C. A 0.5 MacFarland bacterial suspension containing 0.5×10^8 cells/mL was prepared for further downstream processing [25]. A working suspension of 112 µg/mL for each type of Ag-NP was prepared; 100 µL of each suspension was distributed in each well using the double dilution approach; the final concentration was between 0.43 and 112 µg/mL. Subsequently, 100 µL of 0.5 MacFarland bacterial suspension was added in each well. Polymyxin B was used as a positive control; no Ag-NPs were placed in the test control. The microtiter plate was incubated at 37 °C for 24 h; visual demonstration of complete bacterial inhibition (i.e., a visually clear well) was recorded as the MIC. Subsequently, a 5 µL suspension from the plate was sub-cultured on the MHA plates for 24 h; bacterial growth on the plate was subsequently observed. The MBC was determined as the concentration of Ag-NPs for which no growth was observed on sub-cultured plates.

Fluorescence spectroscopic studies

All of the fluorescence (2D and 3D) spectroscopic studies were carried out on a F-7000 fluorescence spectrophotometer (Hitachi, Tokyo, Japan) in ultra-purified water.

Determination of dynamic quenching of fluorophore fluorescein by PEI-capped Ag-NPs

An aqueous solution of fluorescein (10 µm) was prepared; emission spectra at an excitation wavelength of 450 nm (EEM 450–510 nm for 3D spectra) were recorded, followed by the addition of an aqueous suspension of PEI-capped Ag-NPs (20 µL of 5 µg/mL solution). In the same suspension, 10^4 cells *of A. baumannii* (log-phase cells, washed two times with sterile purified water) were added and incubated for 10 min; 2D and 3D spectra were subsequently recorded. 10^8 cells/mL were subsequently added to the same suspension; the emission spectra were recorded.

Cell surface-expressed protein–Ag-NP interaction and membrane fracture studies

A log-phase culture that was grown in a nutrient broth of *A. baumannii* was centrifuged at 8000 rpm for 6 min; it was then washed two to three times with sterile purified water and adjusted to a concentration of 10^4 cells/mL in water. Intrinsic fluorescence spectra of the surface-expressed proteins were recorded using excitation/emission matrix spectroscopy at 280 and 300 nm. All of the as-prepared Ag-NPs were incubated with 10^4 cells/mL. MICs were recorded for 1 or 3 h in three different tubes; fluorescence spectra were obtained using 2D and 3D EEM. Data were obtained using bovine serum albumin (2 µg/mL) in the same manner as cells. All of the PEI-functionalized Ag-NPs were incubated at the corresponding MBC with 10^6 cells/mL for 6 h at room temperature. After 6 h, the cell suspensions were centrifuged for 10,000 rpm for 6 min. The supernatant was collected; 2D fluorescence spectra were recorded separately using EEM at 280 and 300 nm.

References

1. D.R. Radu, C.Y. Lai, K. Jeftinija, E.W. Rowe, S. Jeftinija, and V.S.Y. Lin: A polyamidoamine dendrimer-capped mesoporous silica nanosphere-based gene transfection reagent. *J. Am. Chem. Soc.* **126**, 13216–13217 (2004).

2. D.J. Bharali, I. Klejbor, E.K. Stachowiak, P. Dutta, I. Roy, N. Kaur, E.J. Bergey, P.N. Prasad, and M.K. Stachowiak: Organically modified silica nanoparticles: A nonviral vector for in vivo gene delivery and expression in the brain. *Proc. Natl. Acad. Sci. USA* **102**, 11539–11544 (2005).

3. T. Xia, M. Kovochich, M. Liong, H. Meng, S. Kabehie, S. George, J.I. Zink, and A.E. Nel: Polyethyleneimine coating enhances the cellular uptake of mesoporous silica nanoparticles and allows safe delivery of siRNA and DNA constructs. *ACS Nano* **3**, 3273–3286 (2009).

4. C. Burda, X. Chen, R. Narayanan, and M.A. El-Sayed: Chemistry and properties of nanocrystals of different shapes. *Chem. Rev.* **105**, 1025–1102 (2005).

5. J.R. Morones, J.L. Elechiguerra, A. Camacho, K. Holt, J.B. Kouri, J.T. Ramírez, and M.J. Yacaman: The bactericidal effect of silver nanoparticles. *Nanotechnology* **16**, 2346 (2005).

6. M.A. Radzig, V.A. Nadtochenko, O.A. Koksharova, J. Kiwi, V.A. Lipasova, and I.A. Khmel: Antibacterial effects of silver nanoparticles on gram-negative bacteria: Influence on the growth

and biofilms formation, mechanisms of action. *Coll. Surf. B: Biointerfaces* **102**, 300–306 (2013).

7. G. Franci, A. Falanga, S. Galdiero, L. Palomba, M. Rai, G. Morelli, and M. Galdiero: Silver nanoparticles as potential antibacterial agents. *Molecules* **20**, 8856–8874 (2015).

8. M. Rai, A. Yadav, and A. Gade: Silver nanoparticles as a new generation of antimicrobials. *Biotechnol. Adv.* **27**, 76–83 (2009).

9. B. Wiley, Y. Sun, B. Mayers, and Y. Xia: Shape-controlled synthesis of metal nanostructures: The case of silver. *Chem. Eur. J.* **11**, 454–463 (2005).

10. M. Raffi, F. Hussain, T.M. Bhatti, J.I. Akhter, A. Hameed, and M.M. Hasan: Antibacterial characterization of silver nanoparticles against *E. coli* ATCC-15224. *J. Mater. Sci. Technol.* **24**, 192–196 (2008).

11. T.C. Dakal, A. Kumar, R.S. Majumdar, and V. Yadav: Mechanistic basis of antimicrobial actions of silver nanoparticles. *Front. Microbiol.* **7**, 1831 (2016).

12. P.C. Pandey, G. Pandey, and R.J. Narayan: Controlled synthesis of polyethylenimine coated gold nanoparticles: Application in glutathione sensing and nucleotide delivery. *J. Biomed. Mater. Res. B* **105**, 1191–1199 (2017).

13. R.K. Matharu, L. Ciric, G. Ren, and M. Edirisinghe: Comparative study of the antimicrobial effects of tungsten nanoparticles and tungsten nanocomposite fibres on hospital acquired bacterial and viral pathogens. *Nanomaterials* **10**, 1017 (2020).

14. R.K. Matharu, H. Porwal, L. Ciric, and M. Edirisinghe: The effect of graphene–poly (methyl methacrylate) fibres on microbial growth. *Interf. Focus* **8**, 20170058 (2018).

15. T. Shi, Q. Wei, Z. Wang, G. Zhang, X. Sun, and Q.Y. He: Photocatalytic protein damage by silver nanoparticles circumvents bacterial stress response and multidrug resistance. *mSphere* **4**, e00175-19 (2019).

16. M.K. Rai, S.D. Deshmukh, A.P. Ingle, and A.K. Gade: Silver nanoparticles: the powerful nanoweapon against multidrug-resistant bacteria. *J. Appl. Microbiol.* **112**, 841–852 (2012).

17. Q.L. Feng, J. Wu, G.Q. Chen, F.Z. Cui, T.N. Kim, and J.O. Kim: A mechanistic study of the antibacterial effect of silver ions on *Escherichia coli* and *Staphylococcus aureus*. *J. Biomed. Mater. Res.* **52**, 662–668 (2000).

18. Y. Matsumura, K. Yoshikata, S.I. Kunisaki, and T. Tsuchido: Mode of bactericidal action of silver zeolite and its comparison with that of silver nitrate. *Appl. Environ. Microbiol.* **69**, 4278–4281 (2003).

19. B. Huang, Z.B. Wei, L.Y. Yang, K. Pan, and A.J. Miao: Combined toxicity of silver nanoparticles with hematite or plastic nanoparticles toward two freshwater algae. *Environ. Sci. Technol.* **53**, 3871–3879 (2019).

20. Y. Choi, H.A. Kim, K.W. Kim, and B.T. Lee: Comparative toxicity of silver nanoparticles and silver ions to *Escherichia coli*. *J. Environ. Sci.* **66**, 50–60 (2018).

21. P. Li, J. Li, C. Wu, Q. Wu, and J. Li: Synergistic antibacterial effects of β-lactam antibiotic combined with silver nanoparticles. *Nanotechnology* **16**, 1912 (2005).

22. J.M. Andrews: Determination of minimum inhibitory concentrations. *J. Antimicrob. Chemotherap.* **48**, 5–16 (2001).

23. J. Cavaleri, D. Rankin, J. Harbeck, L.R. Sautter, S.Y. McCarter, S.E. Sharp, H.J. Ortez, and A.C. Spiegel: *Manual of Antimicrobial Susceptibility Testing* (American Society for Microbiology, Washington, 2005); pp. 42–53.

24. K.Y. Lau, N.S. Zainin, F. Abas, and Y. Rukayadi: Antibacterial and sporicidal activity of Eugenia polyantha Wight against *Bacillus cereus* and *Bacillus subtilis*. *Int. J. Curr. Microbiol. Appl. Sci.* **3**, 499–510 (2014).

25. J. McFarland: The nephelometer: An instrument for estimating the number of bacteria in suspensions used for calculating the opsonic index and for vaccines. *J. Am. Med. Assoc.* **49**, 1176–1178 (1907).